

Supporting Information

| | |
|---|----|
| Materials | 3 |
| Synthesis of 2PAP-SAM [(2-(1,3-dioxisoindolin-2-yl)ethyl)phosphonic acid] | 3 |
| Figure S1: Hydrolysis of Et ₂ PAP to afford 2PAP-SAM | 3 |
| Figure S2: ¹ H NMR spectrum of 2PAP-SAM in DMSO | 4 |
| Figure S3: ¹³ C NMR spectrum of 2PAP-SAM in DMSO | 4 |
| Figure S4: ³¹ P NMR spectrum of 2PAP-SAM in DMSO | 5 |
| Figure S5: ASP+ HRMS spectrum of 2PAP-SAM | 5 |
| Figure S6: FT-IR spectrum in ATR mode of 2PAP-SAM as a powder | 6 |
| | |
| Complementary Results | 7 |
| Figure S8: DSC of zinc acetate solution precursors for ZnO film formation. | 7 |
| Table S1: Contact angle, surface free energy and work function values of immersion and spincoated 2PAP-SAM and spincoated IC-SAM | 8 |
| Figure S10: UPS spectra of a) SECO region and b) VBM region of ITO, ZnO, 2PAP-SAM and IC-SAM substrates. | 8 |
| Table S2: Work function comparison between UPS measurement and Kelvin Probe (KP) batch measurement with absolute value of work function of HOPG | 9 |
| Figure S11: Taut plot of ZnO with Optical band gap determination. | 9 |
| Figure S12: KPFM and AFM pictures of ITO, spincoated and immersed 2PAP-SAM. | 10 |
| Figure S13: Structure of the computed SAMs. The red arrows correspond to the orientation of the associated dipole moment vector of two conformers of IC-SAM and 2PAP-SAM. .. | 11 |
| Figure S14: Effect of thickness on the proportion of working ZnO devices. | 11 |
| Figure S15: Effect of thickness on main OPV parameters with ZnO as ETL. | 12 |
| Figure S16: Percentage of working device before (5 batches of 12 cells for each conditions) and after (8 batches) optimisation of active layer deposition and thickness. | 12 |
| Figure S17: Evolution of main parameters of organic solar cells depending on 2PAP-SAM concentration. | 13 |
| Table S3: Organic solar cells devices comparison between ZnO, ITO and ZnO+SAM main parameters measured under illumination of AM 1.5G (100 mW.cm ⁻²) | 13 |
| Figure S18: Current density-voltage curves of organic solar cells devices comparison between ZnO, ITO and ZnO+SAM measured under illumination of AM 1.5G (100 mW.cm ⁻²) | 14 |
| Figure S19 : Evolution of PCE of cells with different ETL (ZnO, ITO, ITO+2PAP-SAM, ITO+IC-SAM) during ageing in dark protected environment. | 14 |

| | |
|--|----|
| Figure S20: Evolution of main parameters statistics of cells with different ETL (ZnO, ITO, ITO+2PAP-SAM, ITO+IC-SAM) during ageing dark in protected environment. | 15 |
| Figure S21: Evolution of main parameters of encapsulated cells with different ETL (ZnO, ITO, ITO+2PAP-SAM, ITO+IC-SAM) during ageing in light with UV filter at 400nm. ... | 16 |
| Figure S22: Evolution of absorbance of PTQ10:Y6 blend film cast over different ETL (ITO, 2PAP-SAM, IC-SAM and ZnO+SAM) during photo oxidation ageing measurement..... | 16 |
| Figure S23: Evolution of main parameters of encapsulated cells with different ETL (ZnO, ITO, 2PAP-SAM, IC-SAM and ZnO+SAM) during ageing in light with UV filter at 400nm. | 17 |
| Figure S24: Survey spectra and main signals of ZnO and 2PAP-SAM deposited onto ITO substrates. | 17 |
| Figure S25: XPS spectra Zn 2p _{3/2} peak for ZnO before and after 72h illumination in dark and protected environment. | 18 |
| Figure S26: XPS spectra of C1s and Zn 2p _{3/2} peak for ZnO and 2PAP-SAM before and after 72h illumination in dark and protected environment. For C1s peak, contribution of different energies (LA model) was added. | 18 |

Materials

All chemicals and solvents are of reagent grade. [diethyl (1,3-dioxoisindolin-2-yl)ethylphosphonate] (Et₂PAP), bromotrimethylsilane (Me₃SiBr), dry Dichloromethane (DCM), and tetrahydrofuran (THF) were obtained from Sigma Aldrich. Nuclear magnetic resonance (NMR) spectra were recorded on a Bruker 400 MHz in deuterated chloroform or dimethylsulfoxide and referenced to tetramethyl silane (TMS). MS spectra were obtained on a Synapt G2-S from Waters with a quadrupole cell collision. Column chromatography purifications were carried out using a Büchi Reveleris X2 Flash Chromatography System on cartridges containing a stationary phase such as 40-63µm silica.

Synthesis of 2PAP-SAM [(2-(1,3-dioxoisindolin-2-yl)ethyl)phosphonic acid]

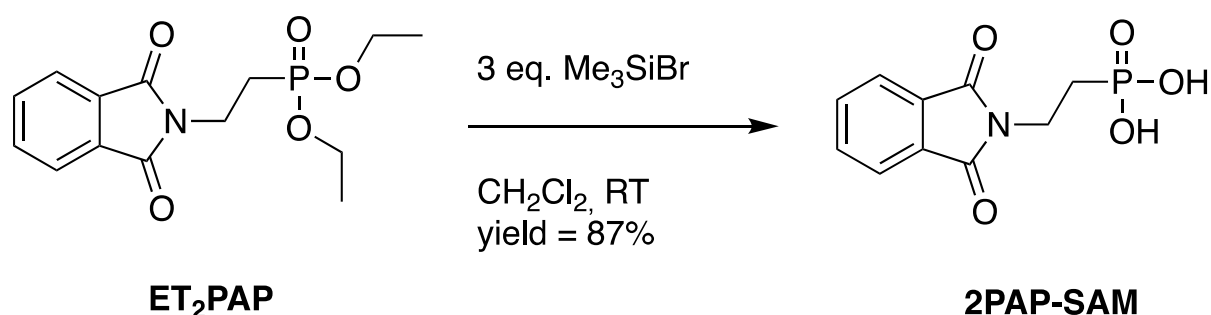


Figure S1: Hydrolysis of Et₂PAP to afford 2PAP-SAM

To a solution of 1 g (3.212 mmol, 1 eq.) of Et₂PAP in 25 mL of dry DCM in two necks round bottom flask under inert atmosphere were added 1.48 g of Me₃SiBr (10 mmol, 3 eq.). The reaction mixture was stirred at room temperature for 22 hours while taking a yellow colour. The dichloromethane was removed under reduced pressure to give a viscous solid in a yellow oil. ¹H NMR realized on the crude revealed the presence of the desired product and a side product bearing a Me₃Si function. Recrystallisation from 50 mL of toluene afforded 920 mg of a white solid collected by filtration. The solid was subsequently dried under vacuum in a desiccator to give 710 mg of 2PAP-SAM (2.78 mmol, yield 87%).

Figure S2: ¹H NMR (400 MHz, DMSO) δ: 9.63 (br, 2H), 8.08 (m, 4H), 3.99 (m, 2H), 2.18 (m, 2H);

Figure S3: ¹³C NMR (100 MHz, DMSO) δ: 167.57, 134.29, 131.77, 122.97, 32.70, 26.79 (d, J = 133 Hz, 1C);

Figure S4: ³¹P (162 MHz, DMSO) δ: 21.36 (m, 1P);

Figure S5: MS (ASAP+) m/z(M+H) = obsd 256.0373, calc 256.0369;

Figure S6: FTIR-ATR: (σOH, 3008,2 cm⁻¹).

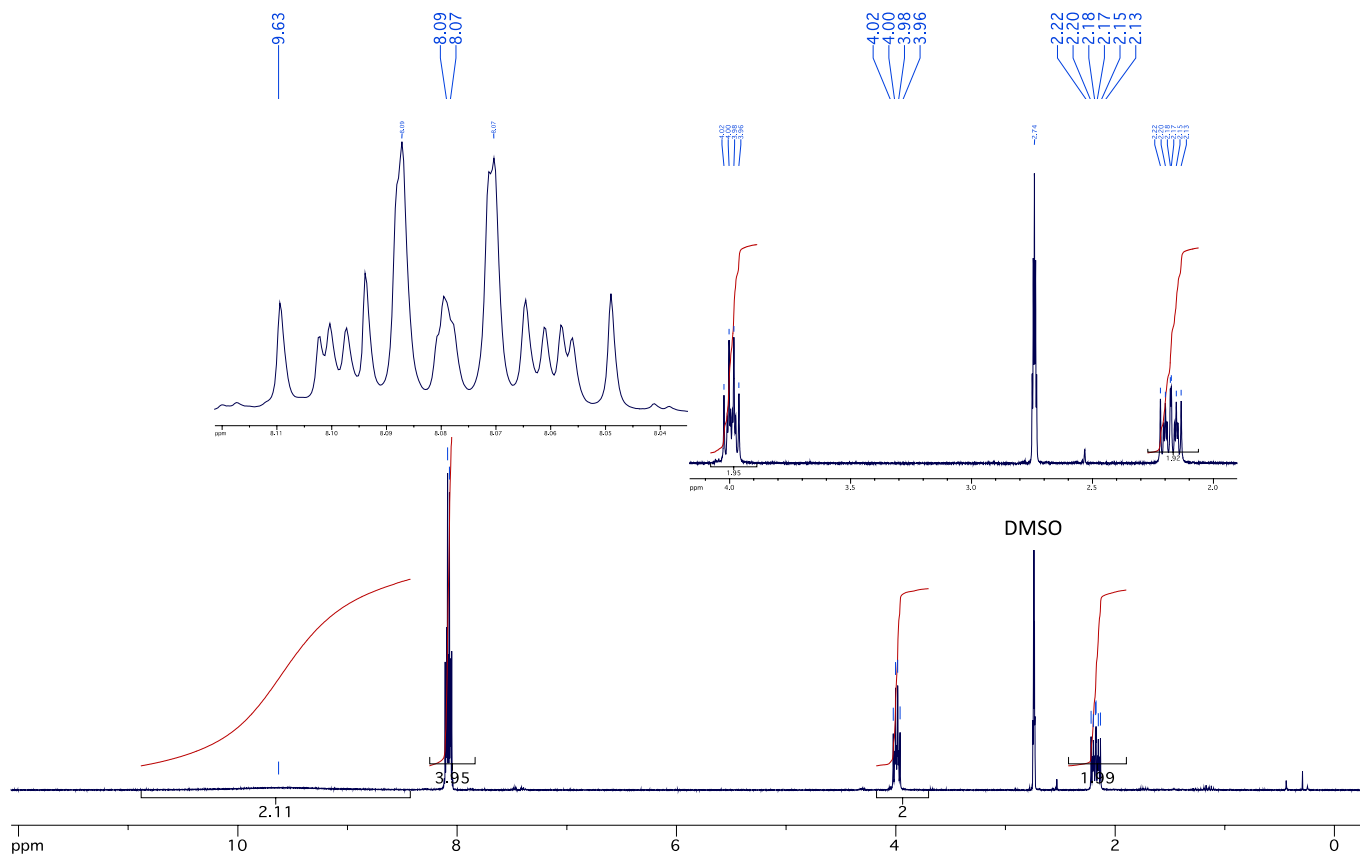


Figure S2: ^1H NMR spectrum of 2PAP-SAM in DMSO.

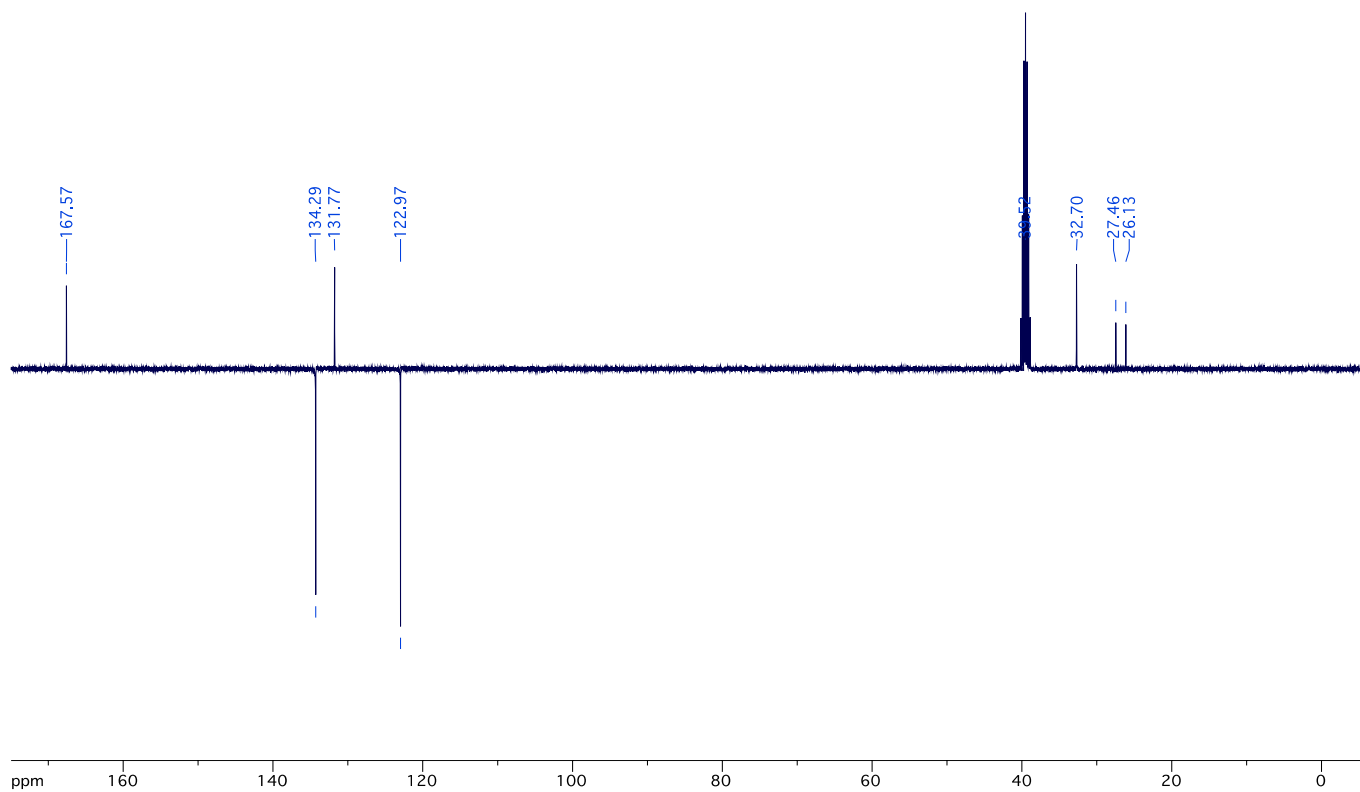


Figure S3: ^{13}C NMR spectrum of 2PAP-SAM in DMSO.

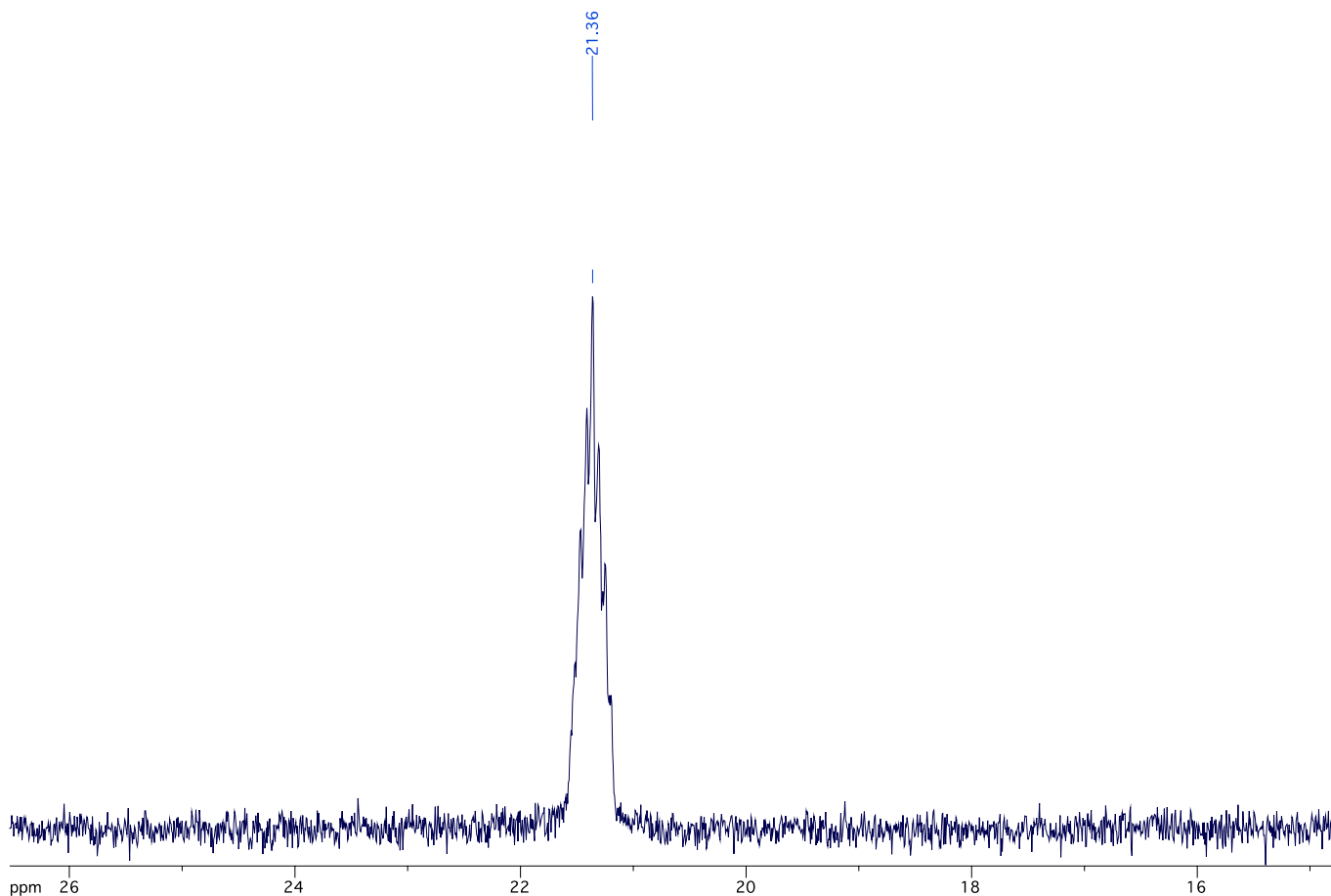
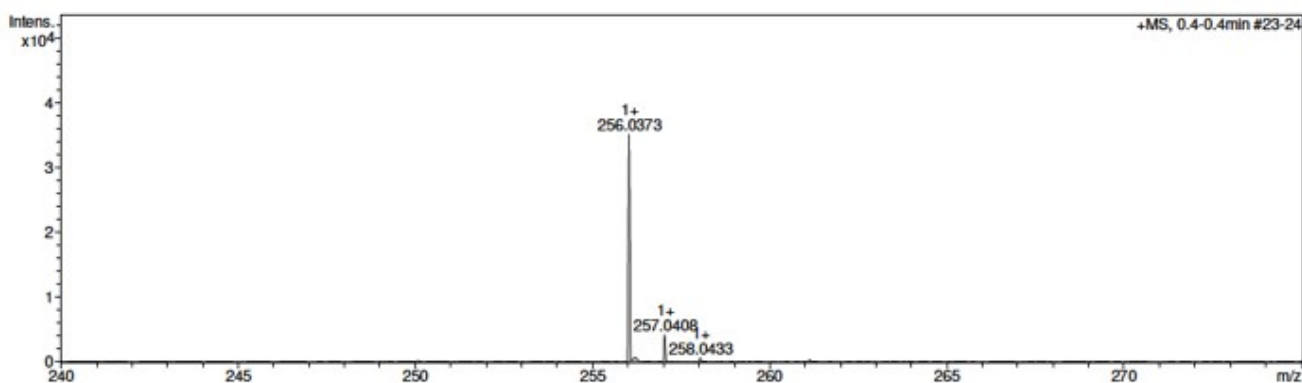


Figure S4: ^{31}P NMR spectrum of 2PAP-SAM in DMSO.

Figure S5: ASP+ HRMS spectrum of 2PAP-SAM.

High Resolution Mass Result

| Analysis Info | | Acquisition Date | 11/9/2023 2:57:53 PM |
|-----------------------|---------------------------|-------------------|-------------------------|
| Sample Name | DAU-7 _ DO-840 pos | Instrument / Ser# | micrOTOF-Q 228888.10300 |
| Acquisition Parameter | | | |
| Source Type | ESI | Ion Polarity | Positive |
| | | Scan Begin | 50 m/z |
| | | Scan End | 3000 m/z |



| Meas. m/z | # | Ion Formula | Score | m/z | err [mDa] | err [ppm] | mSigma | rdb | e ⁻ Conf | N-Rule | Adduct |
|-----------|---|--|--------|----------|-----------|-----------|--------|------|---------------------|--------|--------|
| 256.0373 | 1 | C ₁₀ H ₁₁ NO ₅ P | 100.00 | 256.0369 | 0.3 | 1.3 | 3.2 | 6.5 | even | ok | M+H |
| | 2 | C ₁₁ H ₇ N ₅ O ₄ P | 61.28 | 256.0383 | -1.0 | -3.9 | 11.3 | 11.5 | even | ok | M+H |

Figure S6: FT-IR spectrum in ATR mode of 2PAP-SAM as a powder.

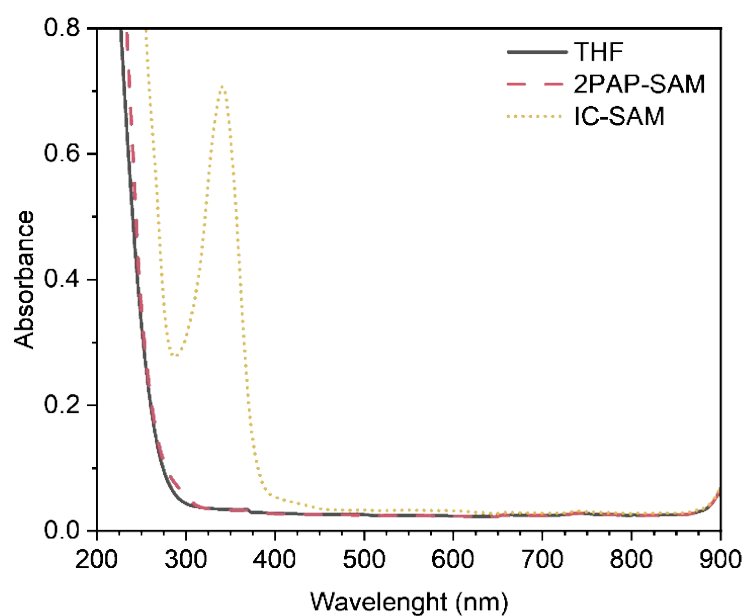
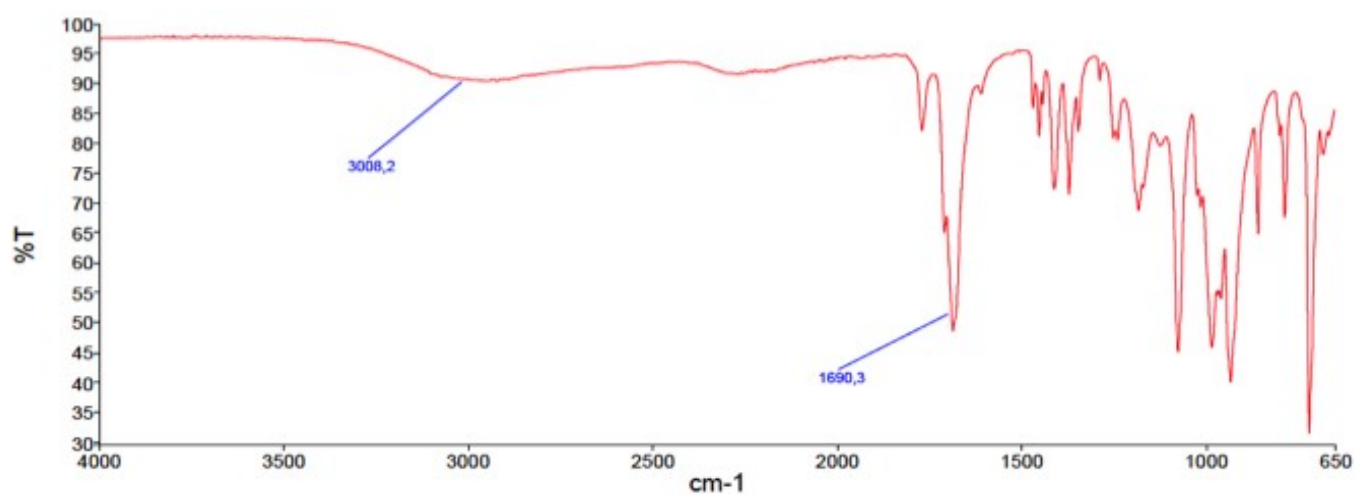


Figure S7: Absorbance spectra of 2PAP-SAM and IC-SAM solution at 2×10^{-5} mol.L⁻¹ in THF.

Complementary Results

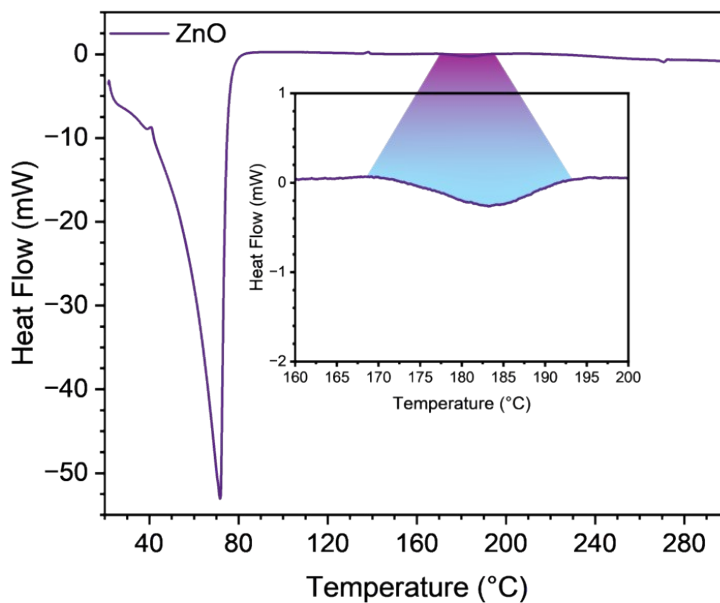


Figure S8: DSC of zinc acetate solution precursors for ZnO film formation.

DSC was performed from 20°C to 300°C with a slope of 2°C/min. After solvent evaporation of ethanol up to 80°C, we observe a small variation of heat flow (integrated to 2.7 J/g) at around 180°C corresponding to formation of oxide, thus justifying the annealing temperature.

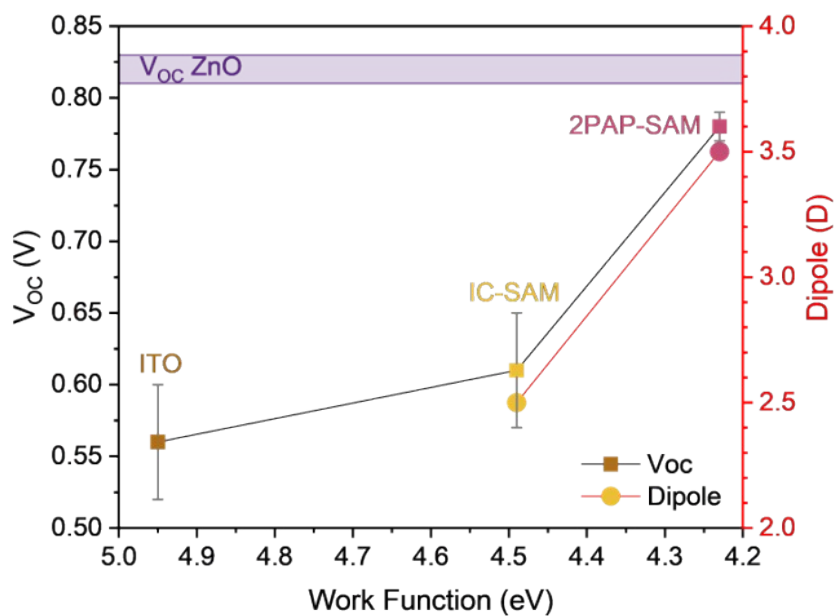


Figure S9: Evolution of Voc depending on work function modification by IC-SAM and 2PAP-SAM and correspondence to molecular dipole.

| Immersion Time (h) | Contact angle with water (°) | Surface Energy (mN/m) | Dispersive component (mN/m) | Polar component (mN/m) | Work Function (eV) |
|----------------------------|------------------------------|-----------------------|-----------------------------|------------------------|--------------------|
| 0 | 14.3 ± 0.9 | 85.0 ± 0.7 | 2.0 ± 0.1 | 83 ± 13 | 5.05 ± 0.04 |
| 1 | 47.4 ± 1.3 | 54.5 ± 2.1 | 5.7 ± 1.1 | 48.8 ± 3.3 | 4.46 ± 0.01 |
| 16 | 50.9 ± 0.4 | 49.7 ± 0.4 | 8.1 ± 0.1 | 41.6 ± 0.5 | 4.34 ± 0.02 |
| 20 | 53.7 ± 0.7 | 46.9 ± 1.1 | 8.8 ± 1.5 | 38.1 ± 2.6 | 4.29 ± 0.08 |
| 24 | 57.2 ± 1.7 | 44.2 ± 2.3 | 7.9 ± 2.1 | 36.3 ± 4.4 | 4.23 ± 0.04 |
| 44 | 55.4 ± 0.5 | 46.9 ± 0.4 | 12.2 ± 0.4 | 32.6 ± 0.8 | 4.27 ± 0.03 |
| 70 | 49.0 ± 0.1 | 52.3 ± 0.3 | 6.5 ± 0.3 | 45.8 ± 0.6 | 4.41 ± 0.02 |
| Spincoated 2PAP-SAM | 50.3 ± 0.2 | 49.0 ± 0.3 | 12.1 ± 1.1 | 36.9 ± 1.4 | 4.35 ± 0.01 |
| Spincoated IC-SAM | 53.42 ± 0.02 | 52.1 ± 1.1 | 2.9 ± 0.7 | 49.2 ± 1.7 | 4.43 ± 0.01 |

Table S1: Contact angle, surface free energy and work function values of immersion and spincoated 2PAP-SAM and spincoated IC-SAM.

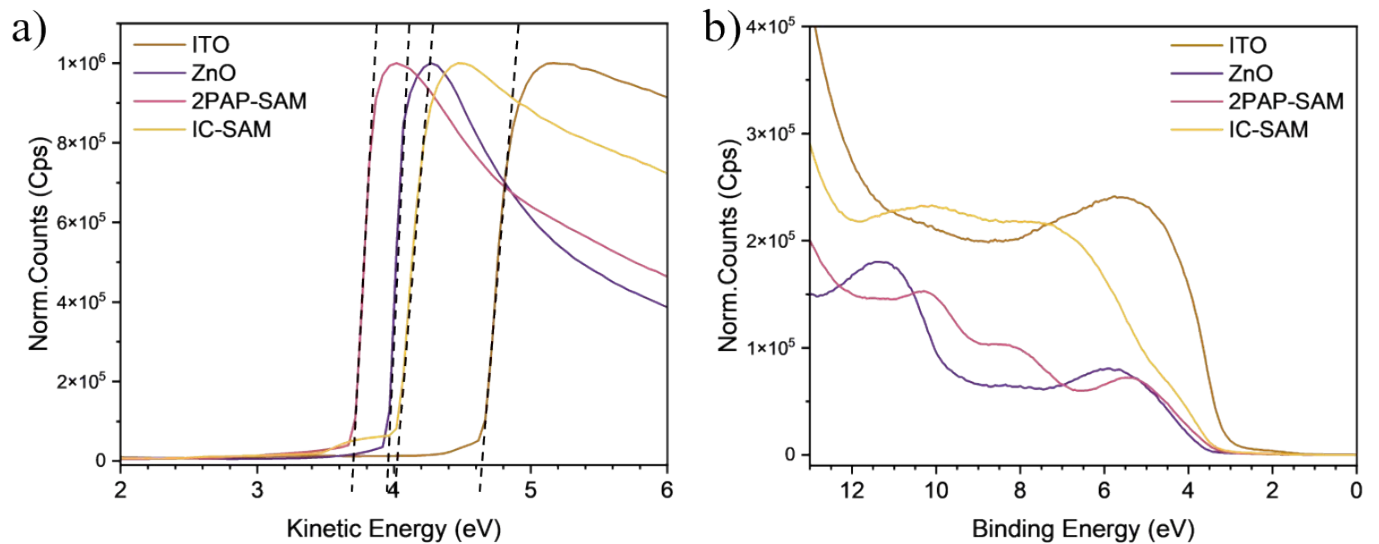


Figure S10: UPS spectra of a) SECO region and b) VBM region of ITO, ZnO, 2PAP-SAM and IC-SAM substrates.

| ETL | WF UPS (eV) | WF KP (eV) | WF KPFM (eV) |
|----------|-------------|-------------|--------------|
| ZnO | 3.96 | 4.36 ± 0.05 | 4.39 ± 0.13 |
| ITO | 4.65 | 4.95 ± 0.15 | 5.08 ± 0.13 |
| 2PAP-SAM | 3.70 | 4.23 ± 0.08 | 4.33 ± 0.11 |
| IC-SAM | 4.00 | 4.49 ± 0.04 | 4.90 ± 0.02 |
| HOPG | 4.43 | / | |

Table S2: Work function comparison between UPS measurement and Kelvin Probe (KP) batch measurement with absolute value of work function of HOPG.

Table S2 and Figure S10 confirm Kelvin Probe trend by showing that 2PAP-SAM induce a greater shift of work function than IC-SAM and pristine cleaned ITO, and comparable to ZnO.

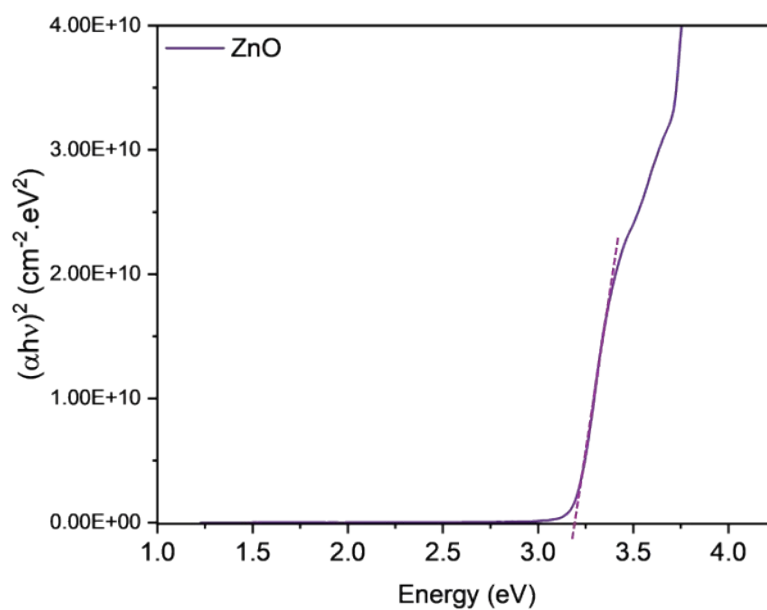


Figure S11: Tauc plot of ZnO with Optical band gap determination.

Optical Band Gap: 3.20 eV ($R^2 = 0.9980$)



Figure S12: KPFM and AFM pictures of ITO, spincoated and immersed 2PAP-SAM.

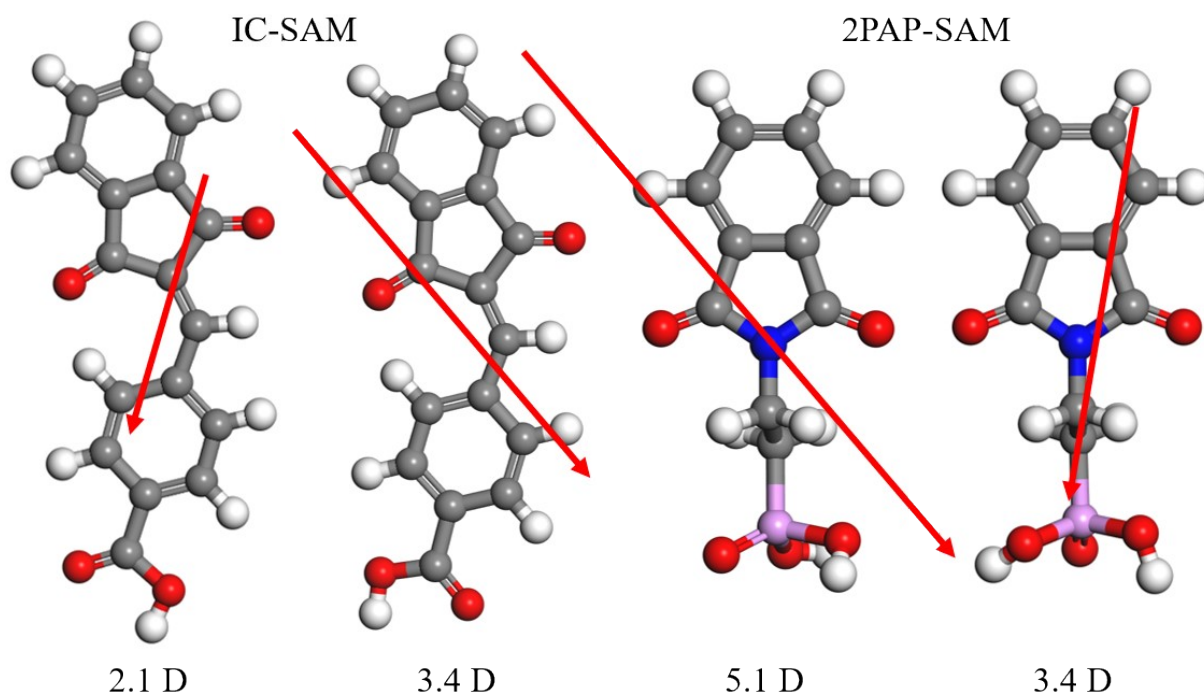


Figure S13: Structure of the computed SAMs. The red arrows correspond to the orientation of the associated dipole moment vector of two conformers of IC-SAM and 2PAP-SAM.

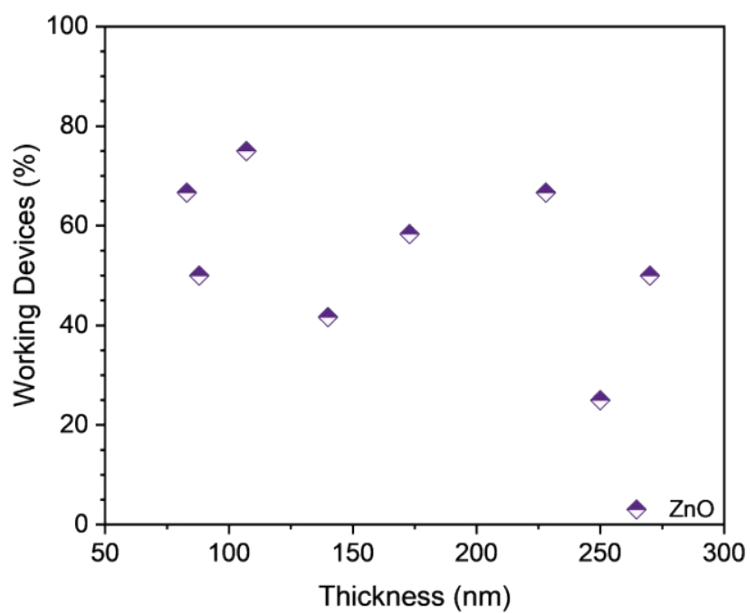


Figure S14: Effect of thickness on the proportion of working ZnO devices.

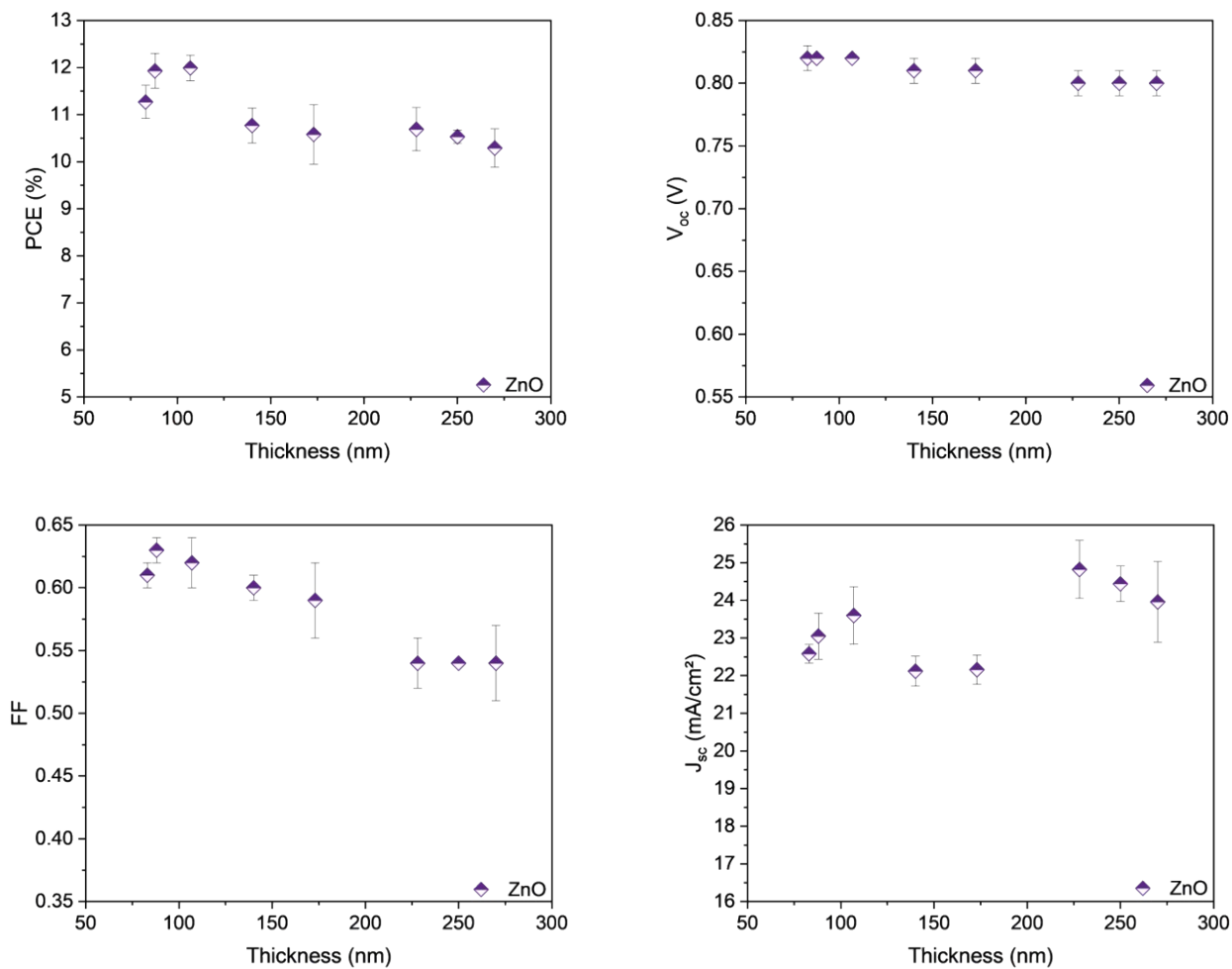


Figure S15: Effect of thickness on main OPV parameters with ZnO as ETL.

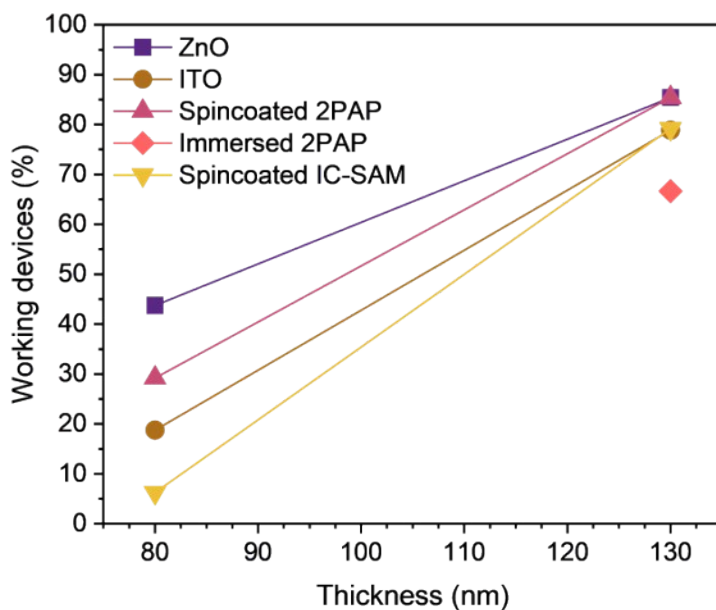


Figure S16: Percentage of working device before (5 batches of 12 cells for each conditions) and after (8 batches) optimisation of active layer deposition and thickness.

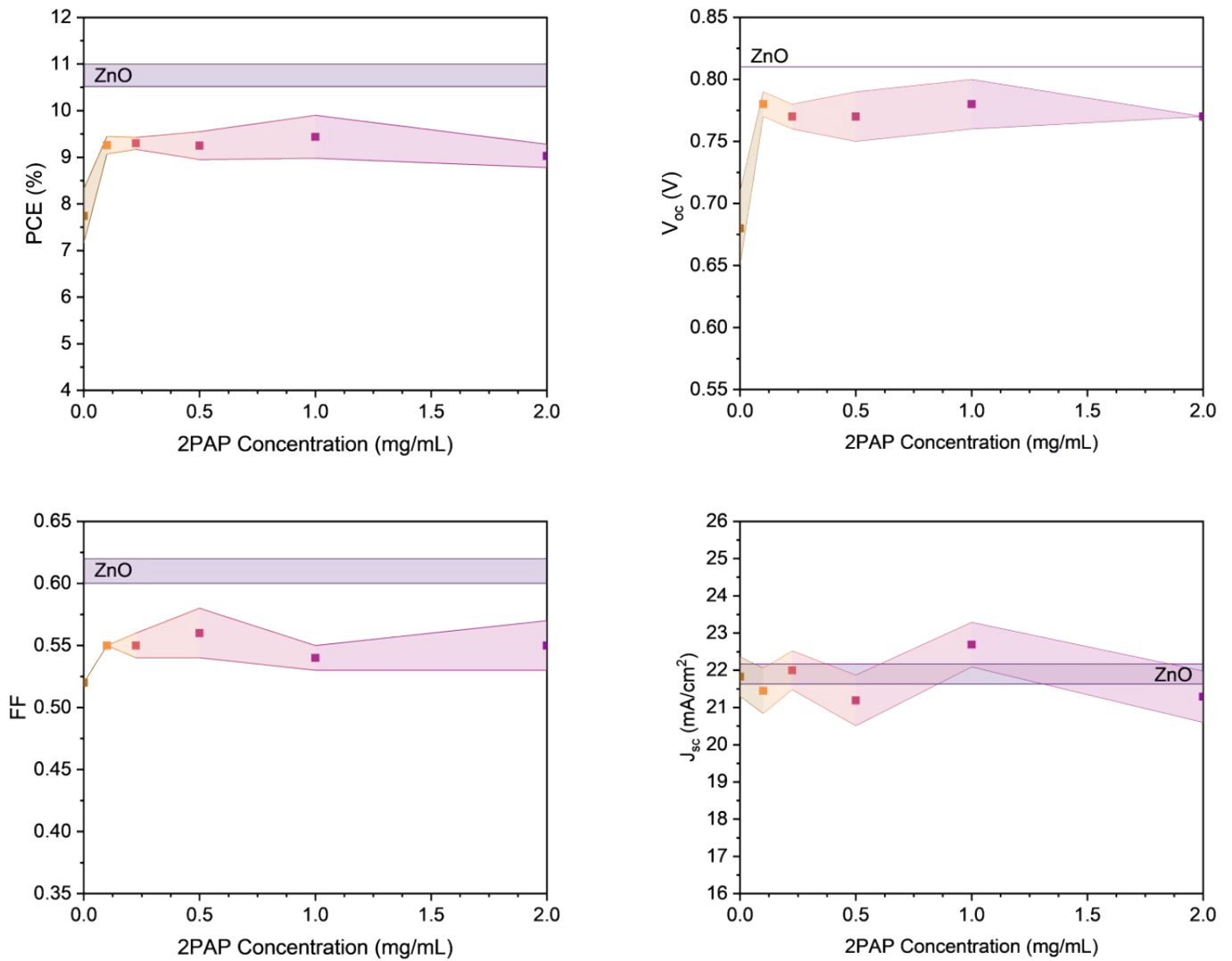


Figure S17: Evolution of main parameters of organic solar cells depending on 2PAP-SAM concentration.

| ETL | J_{SC} (mA/cm ²) | V_{OC} (V) | FF | PCE (%) | Working Devices |
|--------------|--------------------------------|-----------------|-----------------|----------------|-----------------|
| ZnO | 21.5 ± 0.3 | 0.81 ± 0.01 | 0.64 ± 0.01 | 11.1 ± 0.3 | 11/12 |
| ITO | 21.8 ± 0.3 | 0.45 ± 0.04 | 0.50 ± 0.02 | 4.9 ± 0.6 | 3/4 |
| ZnO+2PAP-SAM | 21.6 ± 0.3 | 0.80 ± 0.01 | 0.65 ± 0.01 | 11.3 ± 0.3 | 11/12 |
| ZnO+IC-SAM | 22.0 ± 0.1 | 0.80 ± 0.01 | 0.65 ± 0.01 | 11.5 ± 0.3 | 12/12 |

Table S3: Organic solar cells devices comparison between ZnO, ITO and ZnO+SAM main parameters measured under illumination of AM 1.5G ($100 \text{ mW}\cdot\text{cm}^{-2}$).

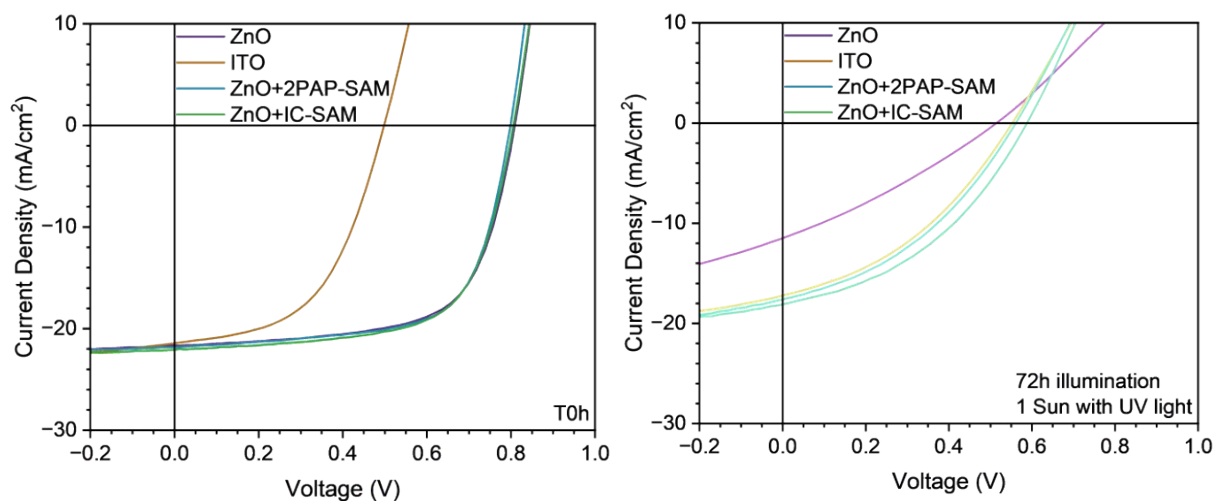


Figure S18: Current density-voltage curves of organic solar cells devices comparison between ZnO, ITO and ZnO+SAM measured under illumination of AM 1.5G ($100 \text{ mW}\cdot\text{cm}^{-2}$).

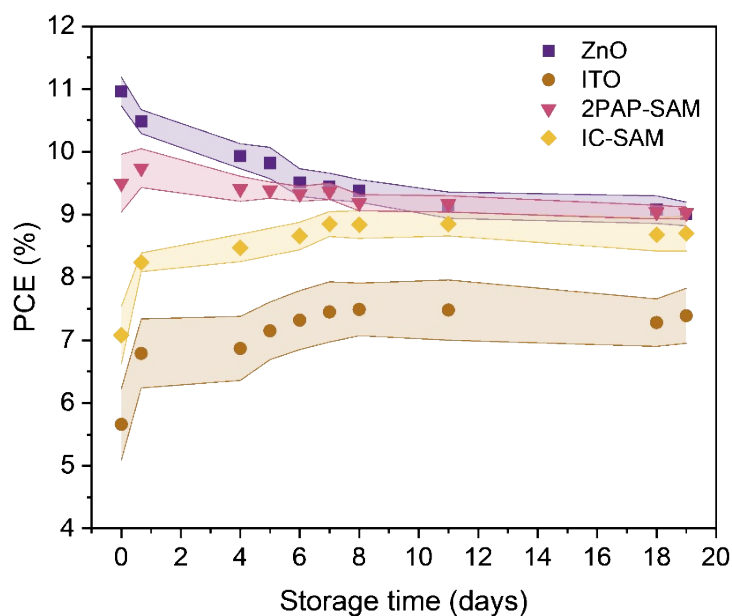


Figure S19 : Evolution of PCE of cells with different ETL (ZnO, ITO, ITO+2PAP-SAM, ITO+IC-SAM) during ageing in dark protected environment.

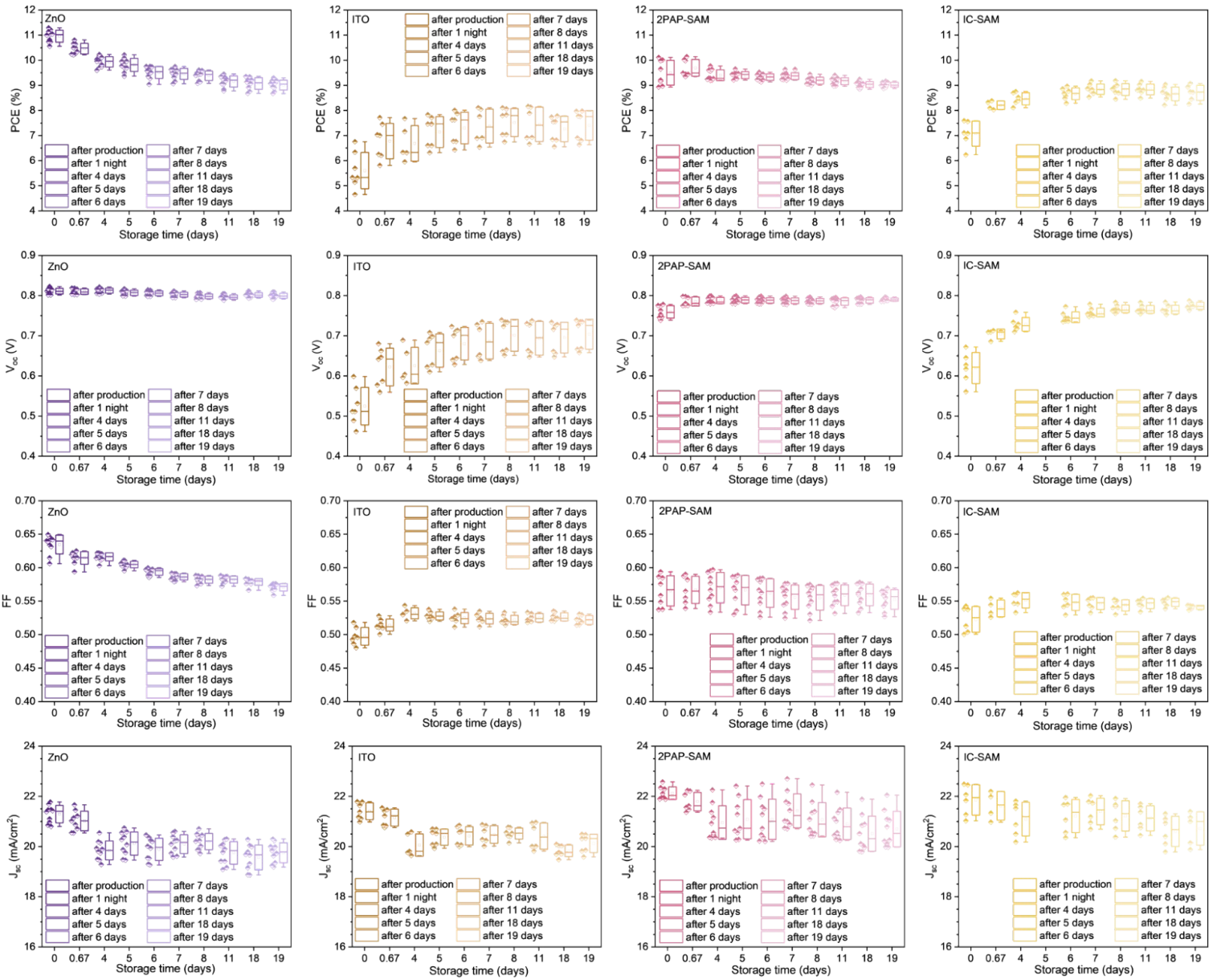


Figure S20: Evolution of main parameters statistics of cells with different ETL (ZnO, ITO, ITO+2PAP-SAM, ITO+IC-SAM) during ageing dark in protected environment.

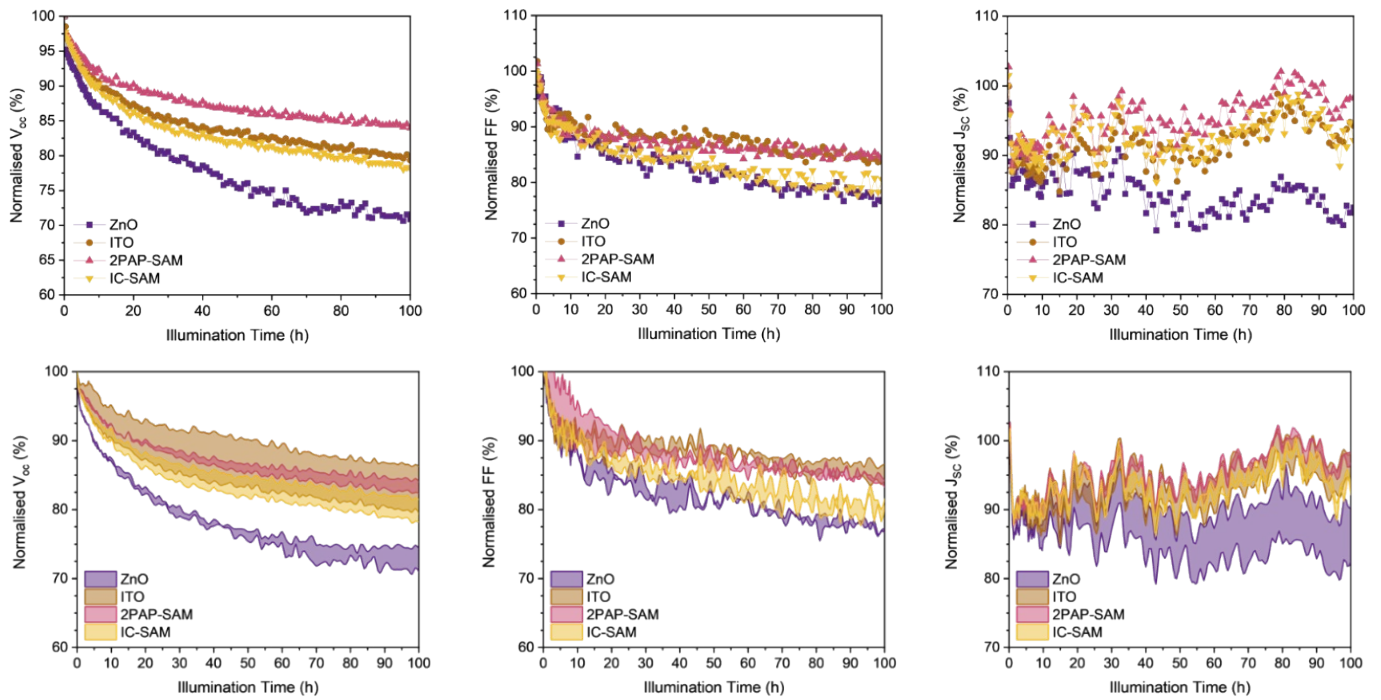


Figure S21: Evolution of main parameters of encapsulated cells with different ETL (ZnO, ITO, ITO+2PAP-SAM, ITO+IC-SAM) during ageing in light with UV filter at 400nm.

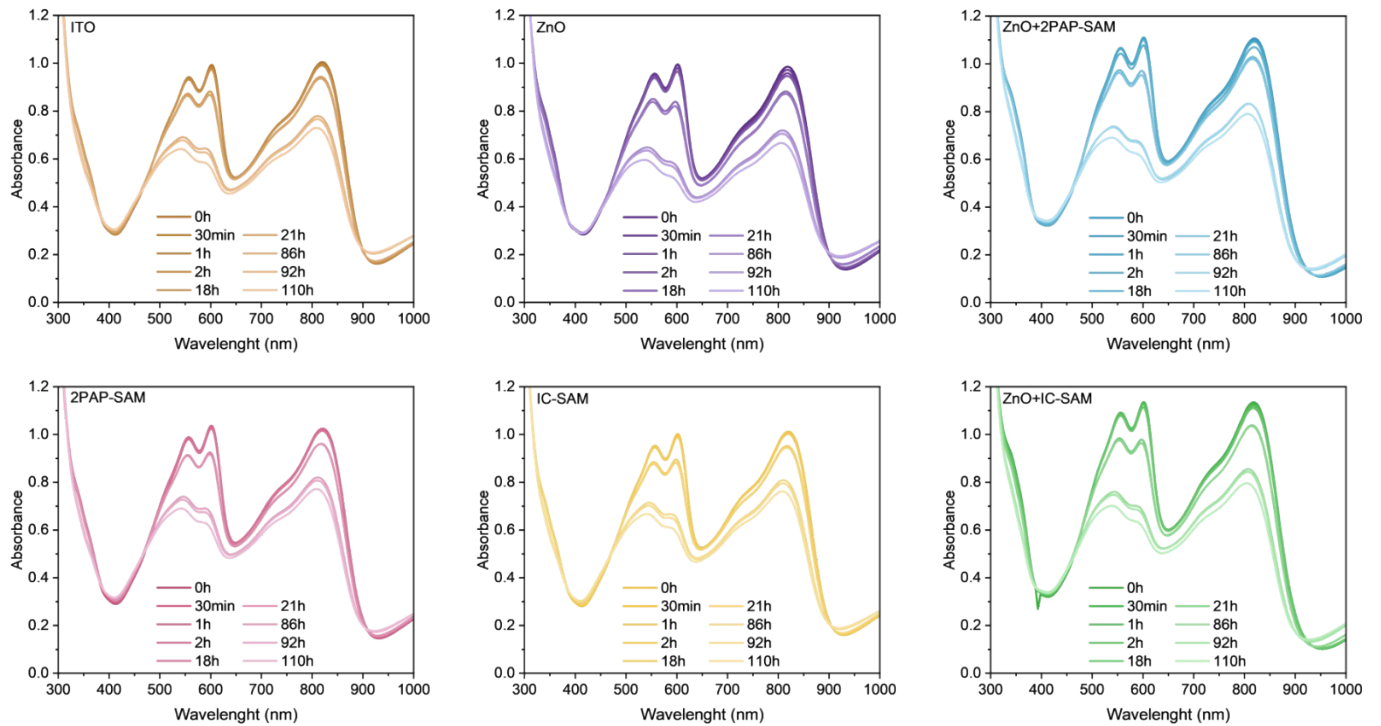


Figure S22: Evolution of absorbance of PTQ10:Y6 blend film cast over different ETL (ITO, 2PAP-SAM, IC-SAM and ZnO+SAM) during photo oxidation ageing measurement.

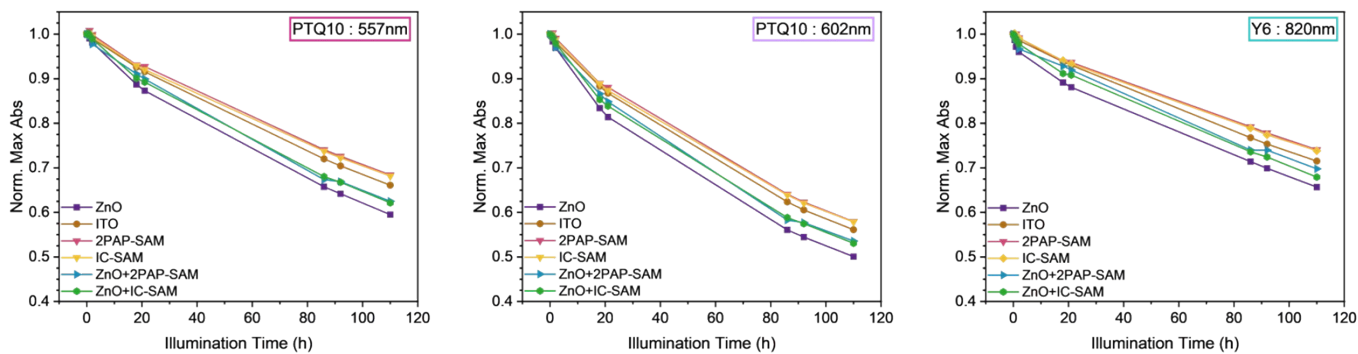


Figure S23: Evolution of main parameters of encapsulated cells with different ETL (ZnO, ITO, 2PAP-SAM, IC-SAM and ZnO+SAM) during ageing in light with UV filter at 400nm.

Figure S22 and Figure S23 shows that SAM grafting onto ZnO reduces loss of absorption and thus degradation of active layer.

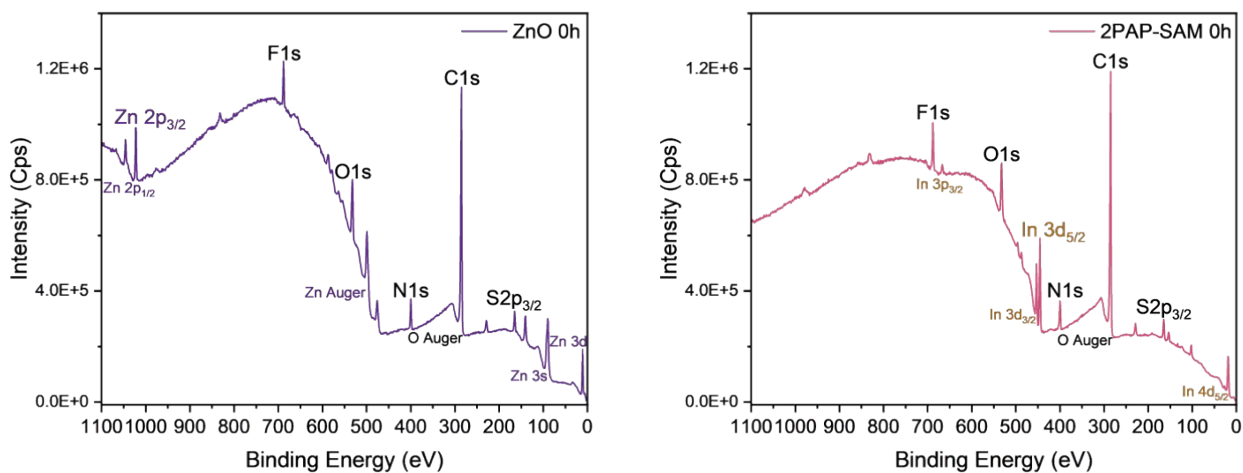


Figure S24: Survey spectra and main signals of ZnO and 2PAP-SAM deposited onto ITO substrates.

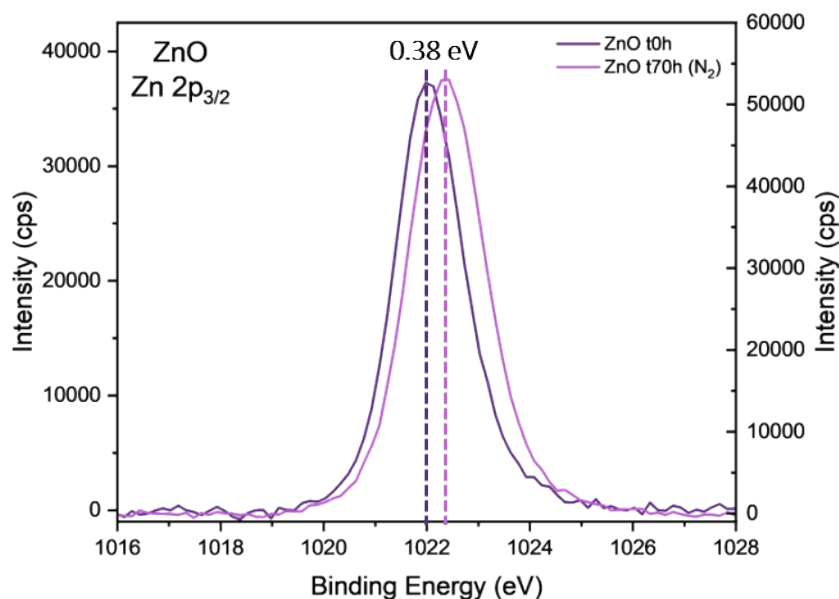


Figure S25: XPS spectra Zn 2p_{3/2} peak for ZnO before and after 70h illumination in dark and protected environment.

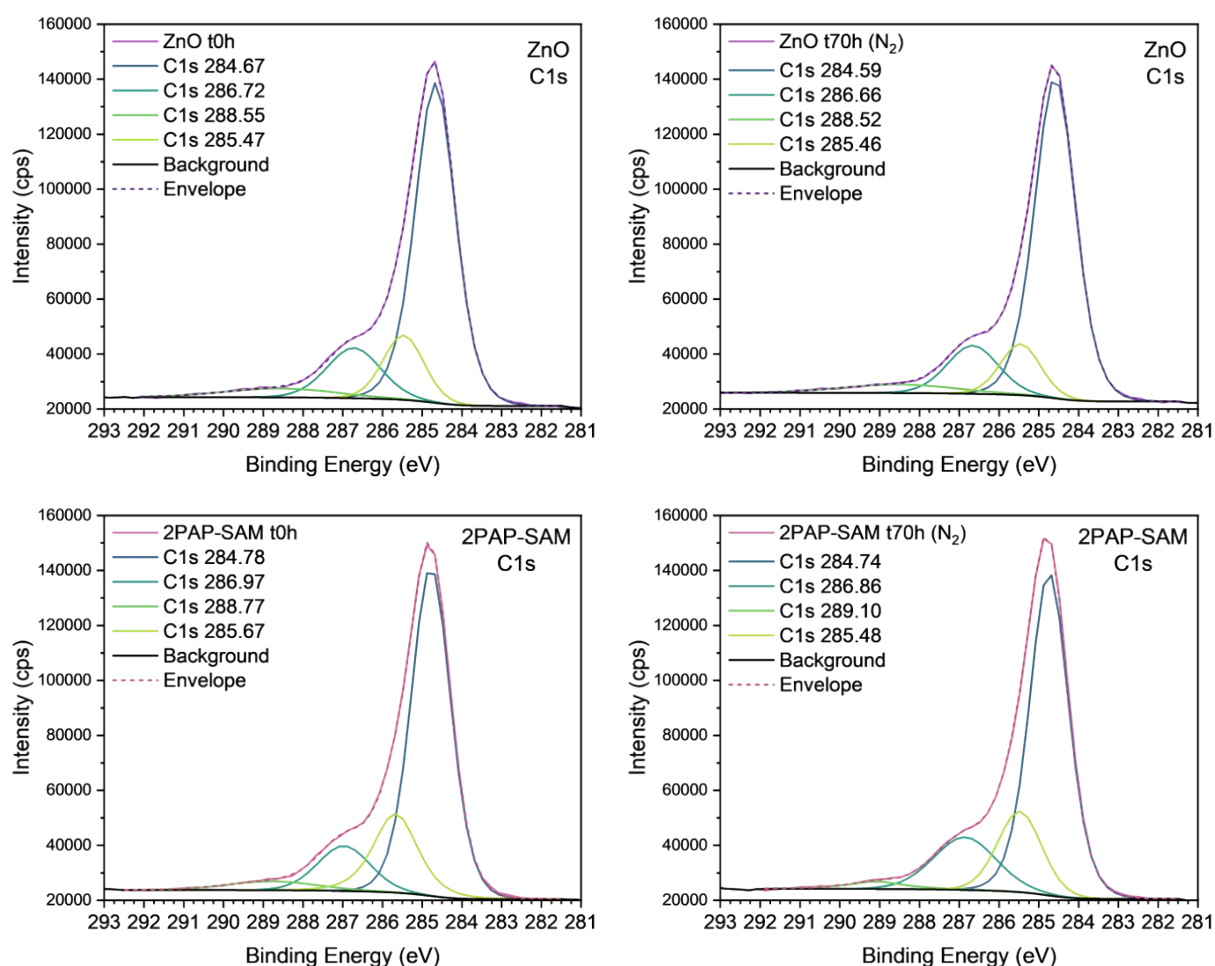


Figure S26: XPS spectra of C1s and Zn 2p_{3/2} peak for ZnO and 2PAP-SAM before and after 70h illumination in dark and protected environment. For C1s peak, contribution of different energies (LA model) was added.